Available free online at www.medjchem.com

Mediterranean Journal of Chemistry **2013**, 2(4), 549-568

Chemical preparation, kinetics of thermal behavior and infrared studies of $Pb_3(P_3O_9)_2.3H_2O$ and $Cd_3(P_3O_9)_2.14H_2O$

Aziz Kheireddine*, Malika Tridane and Said Belaaouad*

Laboratoire de Chimie-Physique Générale des Matériaux. B. P. 7955.
Faculté des Sciences Ben M'sik. Université Hassan II-Mohammedia-Casablanca. Maroc

Abstract: Chemical preparation, thermal behavior, kinetic and IR studies are given for the cyclotriphosphates $Pb_3(P_3O_9)_2.3H_2O$ and $Cd_3(P_3O_9)_2.14H_2O$. The later cyclotriphosphates have never been studied except their crystallographic characterization and are stable in the conditions of temperature and pressure of our laboratory until 343K. The final products of the dehydration and calcination of $Pb_3(P_3O_9)_2.3H_2O$ and $Cd_3(P_3O_9)_2.14H_2O$, under atmospheric pressure, are respectively their long chain polyphosphates, $[Pb(PO_3)_2]_\infty$ and $\beta[Cd(PO_3)_2]_\infty$. The intermediate product of the dehydration of $Cd_3(P_3O_9)_2.14H_2O$, under atmospheric pressure, is its long chain polyphosphate form α, $\alpha[Cd(PO_3)_2]_\infty$. $[Pb(PO_3)_2]_\infty$ and $\beta[Cd(PO_3)_2]_\infty$ are stable until their melting points at respectively 946K and 1153K. Two different methods, Ozawa and KAS have been selected in order to study the kinetics of thermal behavior of the cyclotriphosphates $Pb_3(P_3O_9)_2.3H_2O$ and $Cd_3(P_3O_9)_2.14H_2O$ for the first time. The kinetic and thermodynamic features of the dehydration, of the cited cyclotriphosphates, were determined and discussed on the basis of their crystalline structure. $[Pb(PO_3)_2]_\infty$, $\alpha[Cd(PO_3)_2]_\infty$ and $\beta[Cd(PO_3)_2]_\infty$ have many applications in industry such as corrosion inhibitors.

Keywords: Chemical preparation; cyclotriphosphate; thermal behavior: kinetic study; thermal analyses (TGA-DTA); differential scanning calorimetry (DSC); X-ray diffraction; infrared spectrometry.

Introduction

Bivalent cations cyclotriphosphates $M^{II}_3(P_3O_9)_2.nH_2O$ (M^{II} = Ca, n = 10; M^{II} = Ba, n = 6 and 4; M^{II} = Sr, n =7; M^{II} = Mn, n = 10; M^{II} = Pb, n = 3; M^{II} = Cd, n = 10 and 14) have been studied by their crystalline structures[1-12]. Thermal behaviors, kinetic and IR studies have not yet been investigated for $M^{II}_3(P_3O_9)_2.nH_2O$ (M^{II} = Ba, n = 4; M^{II} = Sr, n =7; M^{II} = Pb, n = 3; M^{II} = Cd, n = 14). The dehydration of these cyclotriphosphates leads generally to long-chain polyphosphates[13,14], $M^{II}(PO_3)_2$ (M^{II} = Ca, Ba, Sr, Pb, Cd) or cyclotetraphosphates[15,16] $M^{II}_2P_4O_{12}$ (M^{II} = Mn, Cd). It is worth noticing that long-chain polyphosphates $M^{II}(PO_3)_2$ can be used in industry such as corrosion inhibitors [17] and humidity sensors[18]. The originality of the cyclotriphosphate $Pb_3(P_3O_9)_2.3H_2O$ is that he's the only cyclotriphosphate crystallizing in the tetragonal system until now to our knowledge. The particularity of these two condensed phosphates is that in the formula type $M^{II}_3(P_3O_9)_2.nH_2O$ (M^{II} = bivalent cations, n = number of water molecules), $Pb_3(P_3O_9)_2.3H_2O$ has the smallest number of water molecules three and $Cd_3(P_3O_9)_2.14H_2O$ has the biggest number of water molecules fourteen.

**Corresponding authors:*
E-mail address: kheireddine.aziz@gmail.com; sbelaaouad@gmail.com
DOI: http://dx.doi.org/10.13171/mjc.2.4.2013.22.05.12

The cyclotriphosphates $Pb_3(P_3O_9)_2.3H_2O$ and $Cd_3(P_3O_9)_2.14H_2O$, presented in this paper are stable under the conditions of temperature and pressure of our laboratory.

The kinetic of thermal dehydration of $Pb_3(P_3O_9)_2.3H_2O$ and $Cd_3(P_3O_9)_2.14H_2O$ was studied using thermal analyses TGA-DTA coupled by two different methods Ozawa and KAS. In this work, the kinetics and thermodynamic parameters for the dehydration process of $Pb_3(P_3O_9)_2.3H_2O$ and $Cd_3(P_3O_9)_2.14H_2O$ are reported for the first time. The present work deals with a synthesis, thermal behavior, kinetic and IR studies of the cyclotriphosphates $Pb_3(P_3O_9)_2.3H_2O$ and $Cd_3(P_3O_9)_2.14H_2O$. It is to be noticed that the results of this paper will be added to previous works on hydrated cyclotriphosphates in order to understand well the mechanism and reactivity of the dehydration of condensed hydrated cyclophosphates.

Results and Discussion

Chemical Preparations

The synthesis of $Pb_3(P_3O_9)_2.3H_2O$ powder consists in slowly mixing $Pb(NO_3)_2$ and $Na_3P_3O_9$ aqueous solutions with a 3:2 at room temperature. The chemical reaction is as follows

$$2Na_3P_3O_9 + 3Pb(NO_3)_2 + 3H_2O \longrightarrow Pb_3(P_3O_9)_2.3H_2O + 6NaNO_3$$

After 10 hours of mechanical stirring, powder of $Pb_3(P_3O_9)_2.3H_2O$ was isolated from the resulting precipitate after filtering. Polycrystalline Samples of the title compound, $Cd_3(P_3O_9)_2.14H_2O$, were prepared by adding slowly dilute cyclotriphosphoric acid to an aqueous solution of cadmium carbonate, according to the following chemical reaction:

$$2H_3P_3O_9 + 3CdCO_3 + 11H_2O \longrightarrow Cd_3(P_3O_9)_2.14H_2O + 3CO_2$$

The so-obtained solution was then slowly evaporated at room temperature until polycrystalline samples of $Cd_3(P_3O_9)_2.14H_2O$ were obtained. The cyclotriphosphoric acid used in this reaction was prepared from an aqueous solution of $Na_3P_3O_9$ passed through an ion-exchange resin "Amberlite IR 120"[19].

Crystal data, chemical analyses and dehydration.

$Pb_3(P_3O_9)_2.3H_2O$ is tetragonal $P4_12_12$ with the following unit-cell dimensions : a = b = 11.957(5)Å, c = 12.270(5)Å and Z = 4[11-12]**.** $Cd_3(P_3O_9)_2.14H_2O$ is hexagonal P-3 with the following unit-cell dimensions : a = b = 12.228(3)Å, c = 5.451 (3)Å and Z = 1[1-3]. $Pb_3(P_3O_9)_2.3H_2O$ and $Cd_3(P_3O_9)_2.14H_2O$ had never been studied except their crystallographic characterizations. The results of the chemical analyses and dehydration of the title compounds are in total accordance with the formula $Pb_3(P_3O_9)_2.3H_2O$ and $Cd_3(P_3O_9)_2.14H_2O$ and are gathered in **Table 1**.

Table 1 Results of the chemical analyses and dehydration of $Pb_3(P_3O_9)_2.3H_2O$ and $Cd_3(P_3O_9)_2.14H_2O$

Stability.

$Cd_3(P_3O_9)_2.14H_2O$		$Pb_3(P_3O_9)_2.3H_2O$	
P/Cd		P/Pb	
Theoretical : 2	Experimental : 2.011	Theoretical : 2	Experimental : 2.001
H_2O		H_2O	
Theoretical : 14	Experimental : 13.97	Theoretical : 3	Experimental : 3

The cyclotriphosphate trihydrate of lead, $Pb_3(P_3O_9)_2.3H_2O$ and the cyclotriphosphate tetradecahydrate of cadmium, $Cd_3(P_3O_9)_2.14H_2O$ are stable in the conditions of temperature and pressure of our laboratory until 343K.

We have followed, by IR spectrometry, X-ray diffraction and thermogravimetric analyses, the stability of $Pb_3(P_3O_9)_2.3H_2O$ and $Cd_3(P_3O_9)_2.14H_2O$ during one year, and no evolution was observed. The X-ray diffraction patterns of $Pb_3(P_3O_9)_2.3H_2O$ and $Cd_3(P_3O_9)_2.14H_2O$ are reported respectively in **Fig. 1** and **2**.

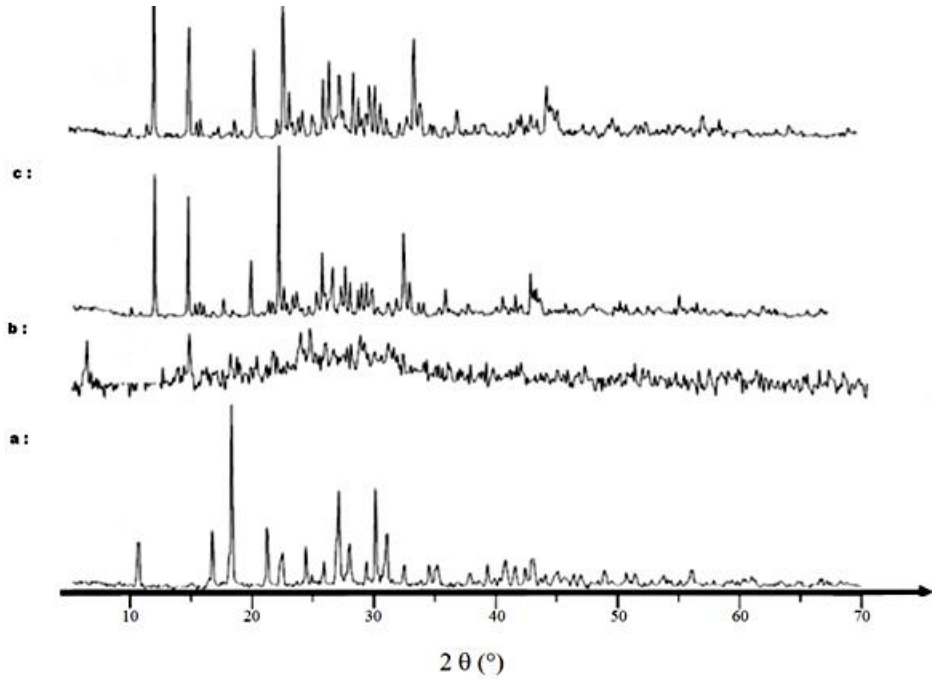

Figure 1. X-ray powder diffractograms of the phosphates (a) $Pb_3(P_3O_9)_2.3H_2O$, (b) amorphous phase, (c) evolution to $[Pb(PO_3)_2]$ and (d) $[Pb(PO_3)_2]$.

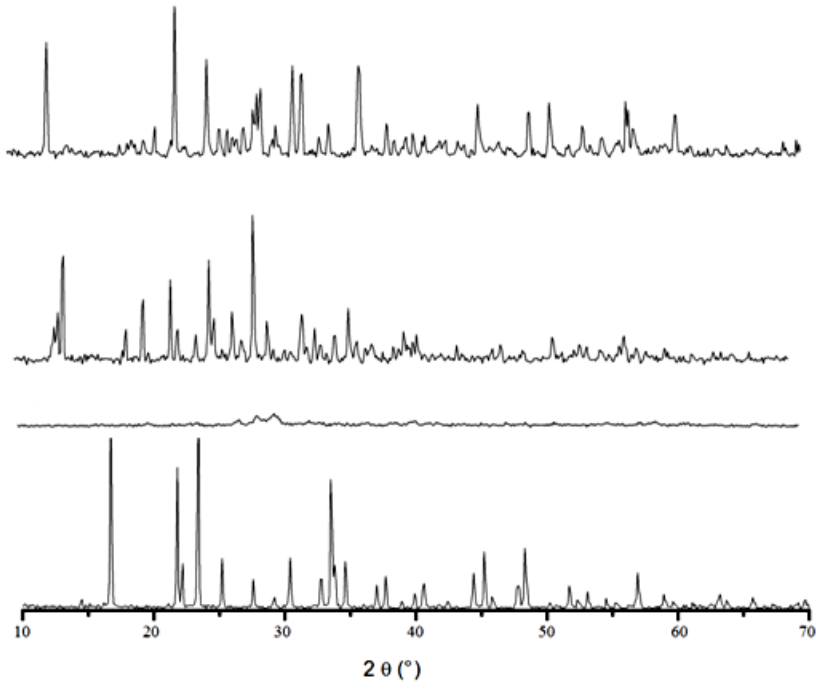

Figure 2. X-ray powder diffractograms of the phosphates (a) $Cd_3(P_3O_9)_2.14H_2O$, (b) amorphous phase, (c) $\alpha[Cd(PO_3)_2]$, (d) $\beta[Cd(PO_3)_2]$

Characterization of $Pb_3(P_3O_9)_2.3H_2O$ and $Cd_3(P_3O_9)_2.14H_2O$ by IR vibration spectrometry.

The IR absorption spectra of $Pb_3(P_3O_9)_2.3H_2O$ and $Cd_3(P_3O_9)_2.14H_2O$ are reported in **Fig. 3** and **4**. In the domain 4000-1600 cm^{-1}, the spectra (**Fig. 3a, 4a**) show bands which are attributed to the stretching and bending vibrations of water molecules. The stretching vibration bands of water molecules (ν_{OH}) are situated between 4000 and 3000 cm^{-1}. The bending vibration bands of water molecules (δ_{HOH}) exist between 1700 and 1600 cm^{-1}.Between 1340 and 660 cm^{-1} the spectra of $Pb_3(P_3O_9)_2.3H_2O$ and $Cd_3(P_3O_9)_2.14H_2O$ (**Fig. 3a, 4a**) show valency vibration bands characteristic of phosphates with ring anions $P_3O_9^{3-}$ [20-23]. Among these bands we can distinguish : - The vibration bands of the (OPO) end groups at high frequencies: 1180 < ν_{as} OPO < 1340 cm^{-1} and 1060 < ν_s OPO < 1180 cm^{-1};

- The valency vibrations of the (P-O-P) ring groups at : 960 < ν_{as} POP < 1060 cm^{-1} and 660 < ν_s POP < 960 cm^{-1} ;

The valency vibrations of the (POP) ring groups in the spectra (**Fig. 3a, 4a**), are characterized by the presence of a very strong band at 978 cm^{-1} for $Pb_3(P_3O_9)_2.3H_2O$ and at 997 cm^{-1} for $Cd_3(P_3O_9)_2.14H_2O$ which can be attributed, in both cases, to the ν_{as} POP antisymmetric vibrations. On the other hand, the same spectra exhibit an intense band between 700 and 800 cm^{-1} (at 763 and 744 cm^{-1} for $Pb_3(P_3O_9)_2.3H_2O$, 779 and 750 cm^{-1} for $Cd_3(P_3O_9)_2.14H_2O$) which can be related to the ν_s POP symmetric vibrations. The strong bands between 700 and 800 cm^{-1} clearly characterize the structure of a cyclotriphosphate $P_3O_9^{3-}$ [20]. In the spectral domain 660-400 cm^{-1}, the spectra of $Pb_3(P_3O_9)_2.3H_2O$ and $Cd_3(P_3O_9)_2.14H_2O$ (**Fig. 3a, 4a**) show bending vibration bands characteristic of phosphates with ring anions [20-23]. The vibrations corresponding to the different observed bands are given in **Table 2**.

Table 2: Frequencies (cm^{-1}) of IR absorption bands for $Pb_3(P_3O_9)_2.3H_2O$ and $Cd_3(P_3O_9)_2.14H_2O$ and assignments of the stretching vibrations of the $P_3O_9^{3-}$ cycles with approximate symmetry C_{3v}

$Pb_3(P_3O_9)_2.3H_2O$ ν / cm^{-1} This work	$Cd_3(P_3O_9)_2.14H_2O$ ν / cm^{-1}		vibration	Mode
	This work	Ref. 24		
3427		3545	ν OH	
	3519	3500		
1658			ν_δ HOH	
1611	1626	1625		
1261	1306	1265	ν_{as} OPO^-	mode E
1211	1280	1242		mode A_1
1138	1161	1164	ν_s OPO^-	mode A_1
1105	1088	1098		mode E
1066				
978	997	1022	ν_{as} POP	mode E
	852			
763	779	792		mode E
744	750	760	ν_s POP	mode A_1
680	680			
635	625	637	δ OPO+	
		573	ρ OPO	
511	525	518		

Vibrational study of the cyclotriphosphates $Pb_3(P_3O_9)_2.3H_2O$ and $Cd_3(P_3O_9)_2.14H_2O$

The attributions of the stretching frequencies of the $P_3O_9^{3-}$ cycles with approximate symmetry C_{3v} in the cyclotriphosphates $Pb_3(P_3O_9)_2.3H_2O$ and $Cd_3(P_3O_9)_2.14H_2O$ are gathered in **Table 2**. We shall notice that the approximate symmetry or pseudo-symmetry C_{3v} of the P_3O_9 cycles in $Pb_3(P_3O_9)_2.3H_2O$ [1-3]and $Cd_3(P_3O_9)_2.14H_2O$ [11,12] which were determined by X-ray diffraction is a good approximation which make the interpretation of the IR experimental spectra of the title compounds possible. In the IR spectra of this class of compounds analyzed on the basis of the crystalline unit-cell, one must expect to observe 6 frequencies per stretching vibrations in both IR and Raman domains. In all cases, the observed frequencies in the IR spectra do not exceed those predicted theoretically. The IR bands characteristic of a lowering of the symmetry of the P_3O_9 cycle with respect to the symmetry C_{3h} observed around 680 cm^{-1} and 1150 cm^{-1} are observable in the IR spectra of both compounds (680 and 1138 cm^{-1} for $Pb_3(P_3O_9)_2.3H_2O$, 680 and 1161 cm^{-1} for $Cd_3(P_3O_9)_2.14H_2O$). These frequencies are assigned to the simple modes A_1 of the C_{3v} symmetry. They characterize in IR a lowering of symmetry compared to the C_{3h} symmetry and are the most intense frequencies which one can expect in the Raman spectra of all the cyclotriphosphates no matter what the symmetry of their cycle P_3O_9 is.

Step manner study

The thermal behavior of $Pb_3(P_3O_9)_2.3H_2O$ and $Cd_3(P_3O_9)_2.14H_2O$ was also studied in a step manner of temperature by X-ray diffraction and IR absorption spectrometry between 293 and 973K for $Pb_3(P_3O_9)_2.3H_2O$ and 1173K for $Cd_3(P_3O_9)_2.14H_2O$. X-ray diffraction patterns recorded after annealing for 36 hours at different temperatures reveal that $Pb_3(P_3O_9)_2.3H_2O$ and $Cd_3(P_3O_9)_2.14H_2O$ are stable up to 343K (**Fig. 1a**, **2a**). The removal of water molecules of hydration of $Pb_3(P_3O_9)_2.3H_2O$ observed in the temperature range 373-423K and $Cd_3(P_3O_9)_2.14H_2O$ between 343-443, broke the crystalline networks and brings to intermediate amorphous phases [25] which do not diffract the X-ray (**Fig. 1b**), nor exhibit the IR absorption bands characteristic of a cyclic phosphate $P_3O_9^{3-}$ (**Fig. 2b**) [20-23]**.** The amorphous products are, according to Van Wazer [25], probably a mixture of lead oxide PbO and pentoxide phosphorus P_2O_5 for $Pb_3(P_3O_9)_2.3H_2O$ and mixture of cadmium oxide CdO and pentoxide phosphorus P_2O_5 for $Cd_3(P_3O_9)_2.14H_2O$. Generally, when the dehydration of condensed phosphates lead to amorphous and hygroscopic phases, according to Van Wazer [25], the obtained IR spectra and X-Ray diffraction patterns don't allow any identification. It's the case for $Cd_3(P_3O_9)_2.14H_2O$. Concerning $Pb_3(P_3O_9)_2.3H_2O$ the few and weak peaks in X-Ray diffraction don't concern neither P_2O_5 nor PbO. After the removing of the remaining water molecules, the atomic rearrangement of $M^{II}O$ (M^{II} = Pb and Cd) and P_2O_5 occurs and leads the crystallization of long-chain polyphosphates $Pb(PO_3)_2$ [26] and $\alpha[Cd(PO_3)_2]$[27]. The latter result is confirmed by chemical analyses, X-ray diffraction **(Fig. 1c, 1d, 2c)** and IR absorption spectrometry (**Fig. 3c, 3d, 4c**). In fact, the bands appearing in the IR absorption spectra of $Pb_3(P_3O_9)_2.3H_2O$ and $Cd_3(P_3O_9)_2.14H_2O$ (**Fig. 3c, 3d, 4c**), characterize easily the structure of long-chain polyphosphates PO_3^- [20,21]. The intermediate product of the dehydration of $Cd_3(P_3O_9)_2.14H_2O$, between 773 and 1073K under atmospheric pressure, is its long chain polyphosphate form α, $\alpha[Cd(PO_3)_2]_\infty$. The final products of the dehydration, decomposition and calcination of $Pb_3(P_3O_9)_2.3H_2O$ and $Cd_3(P_3O_9)_2.14H_2O$, respectively in the ranges 623-923K and 1103K-1133K, under atmospheric pressure, are their long chain polyphosphates $[Pb(PO_3)_2]$ [26] and $\beta[Cd(PO_3)_2]_\infty$[28] confirmed by X-ray diffraction **(Fig. 1d, 2d)**

and IR absorption spectrometry **(Fig. 3d, 4d).** With further increase in temperature, $[Pb(PO_3)_2]_\infty$ **and β$[Cd(PO_3)_2]_\infty$** melt respectively at 946K and 1153K.

$[Pb(PO_3)_2]$ was prepared, by an other route, using the method of Thilo and Grunze[29]. Stoichiometric quantities of $(NH_4)_2HPO_4$ and $PbCO_3$ are well ground and mixed, and very progressively heated to 673K for the purpose of excluding H_2O, CO_2 and NH_3. The heating is then resumed up to 773K, and this temperature is maintained with intervening grindings until a pure phase is obtained, as checked by X-ray diffractometry and IR absorption Spectrometry. $[Pb(PO_3)_2]_\infty$ was obtained as polycristalline samples. $\alpha[Cd(PO_3)_2]_\infty$ and $\beta[Cd(PO_3)_2]_\infty$ were obtained as polycristalline samples at respectively 1023K and 1123K as described for the case of $[Pb(PO_3)_2]_\infty$.

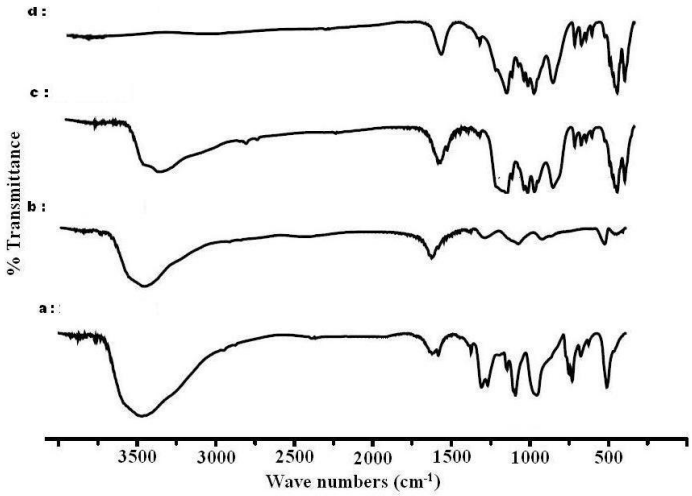

Figure 3. IR spectra of the phosphates (a) $Pb_3(P_3O_9)_2.3H_2O$, (b) amorphous phase, (c) evolution to $[Pb(PO_3)_2]$ and (d) $[Pb(PO_3)_2]$

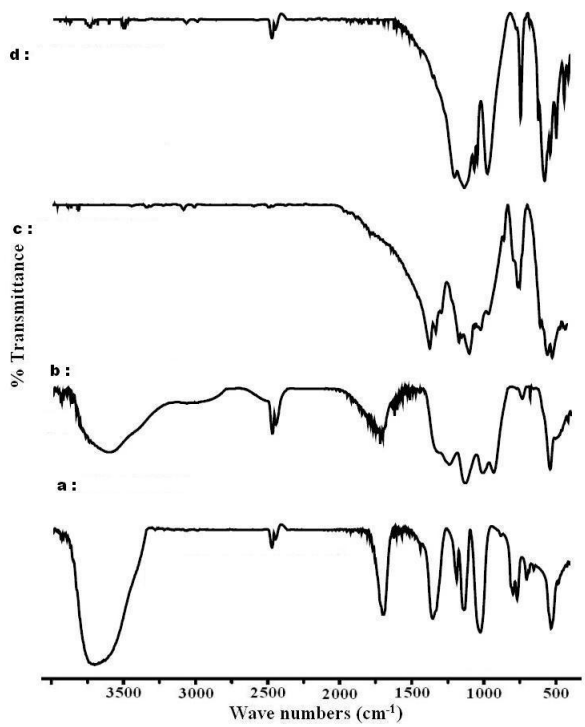

Figure 4. IR spectra of the phosphates (a) $Cd_3(P_3O_9)_2.14H_2O$, (b) amorphous phase, (c) $\alpha[Cd(PO_3)_2]$, (d) $\beta[Cd(PO_3)_2]$

Characterization of $[Pb(PO_3)_2]$, $\alpha[Cd(PO_3)_2]$ and $\beta[Cd(PO_3)_2]$ by IR vibration spectrometry

The IR absorption spectra of $[Pb(PO_3)_2]$, $\alpha[Cd(PO_3)_2]$ and $\beta[Cd(PO_3)_2]$ are reported in **Fig. 3 and 4**. Between 1300 and 650 cm^{-1}, the spectra **(Fig. 3d, 4c and 4d)** show valency vibration bands characteristic of long-chain polyphosphates PO_3^- [20-22]. Among these bands we can distinguish :

- The vibration bands of the (OPO) end groups at high frequencies: $1200 < \nu_{as}$ OPO < 1300 cm^{-1} and $1100 < \nu_s$ OPO < 1170 cm^{-1};
- The valency vibrations of the (P-O-P) chain groups at : $850 < \nu_{as}$ POP < 1050 cm^{-1} and $650 < \nu_s$ POP < 800 cm^{-1};
- The valency vibrations of the (POP) chain groups are represented in the spectra **(Fig. 3d, 4c and 4d)** by a strong band at 913 cm^{-1} for $[Pb(PO_3)_2]$, 919 cm^{-1} for $\alpha[Cd(PO_3)_2]$ and 940 cm^{-1} for $\beta[Cd(PO_3)_2]$ which can be attributed to the ν_{as} POP antisymmetric vibrations. This strong band clearly characterize with no ambiguity the structure of a long-chain polyphosphate PO_3^- [20-22]. By the examination of the position, the profile and the intensity of this band which doesn't appear in the IR spectra of the cyclotriphosphates $P_3O_9^{3-}$ and which is located generally between 850 cm^{-1} and 940 cm^{-1}, it is then possible to distinguish between cyclotriphosphate $P_3O_9^{3-}$ and long-chain polyphosphate PO_3^- [20-22].
- Between 600 and 400 cm^{-1} the spectra **(Fig. 3d, 4c and 4d)** show bending vibration bands characteristic of long-chain polyphosphates[20-22]. The nature of the vibration corresponding to the different observed bands is given in **Table 3**.

Table 3 Frequencies (cm^{-1}) of IR absorption bands for $[Pb(PO_3)_2]$, $\alpha[Cd(PO_3)_2]$ and $\beta[Cd(PO_3)_2]$

$[Pb(PO_3)_2]$	α $[Cd(PO_3)_2]$	β $[Cd(PO_3)_2]$	
ν / cm^{-1}	ν /cm^{-1}	ν /cm^{-1}	vibration
1305 1210	1303 1265 1223		ν_{as} OPO^-
1180 1140 1106	1102	1154	ν_s OPO^-
1077 1039 1013 913	1045 1007 970 919	1096 1030 1007 940	ν_{as} POP
780 739 706 669	816 715	721 666 607	ν_s POP
589 558 541 525 510 462	578 530 497 452	563 528 487 435 407	δ OPO + ρ OPO

Thermal behavior. Non isothermal study.

A. $Pb_3(P_3O_9)_2.3H_2O$

The two curves corresponding to the ATG and DTG analyses in air atmosphere and at a heating rate 5K.min^{-1} for $Pb_3(P_3O_9)_2.3H_2O$ are given in **Fig. 5**. The initial mass is 20mg. The dehydration of the cyclotriphosphate trihydrate of lead, $Pb_3(P_3O_9)_2.3H_2O$, occurs in two steps each one of them within the temperature ranges 430 – 463K and 512 – 654K respectively. In the thermogravimetric (ATG) curve, the first stage between 430 and 463K corresponds to the elimination of 0.22 water molecule and the second stage from 512 to 654K is due to the elimination of 2.78 water molecules.

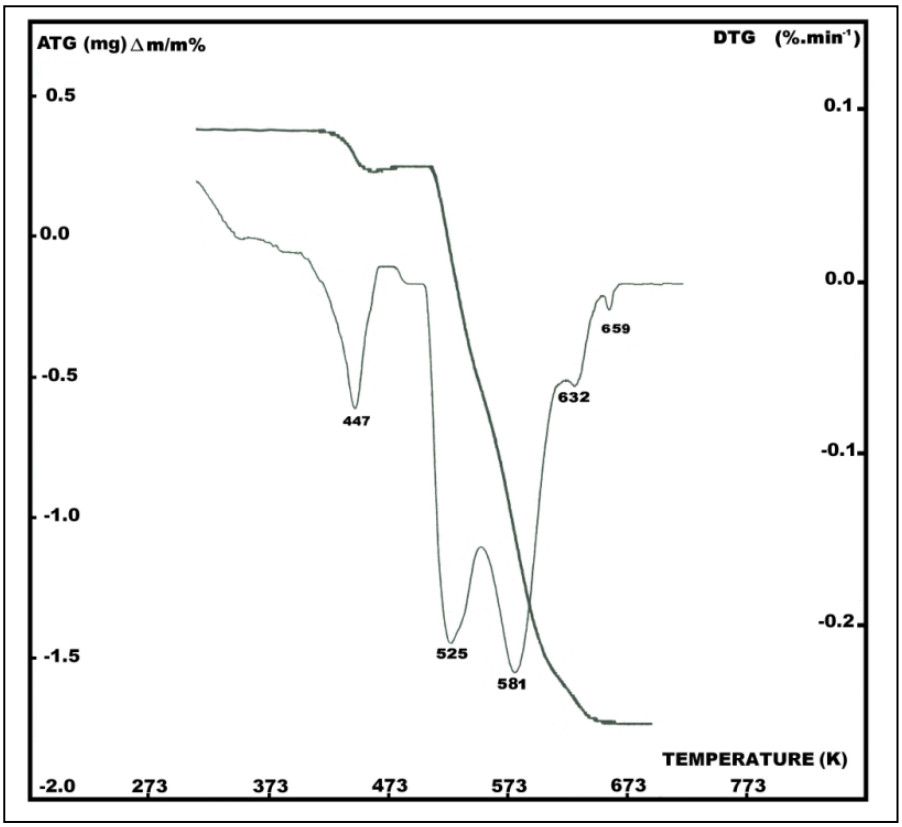

Figure 5. TGA (ATG-DTG) curves of $Pb_3(P_3O_9)_2.3H_2O$ at rising temperature (5K.min^{-1})

The derivative of the ATG curve, DTG, of $Pb_3(P_3O_9)_2.3H_2O$ under atmospheric pressure and at a heating rate of 5K.min^{-1} contains five peaks due to the dehydration of $Pb_3(P_3O_9)_2.3H_2O$. The first peak in the domain 430 – 463K, at 447K is due to the departure of 0.22 water molecule. The second, third, fourth and fifth peaks in the range 512 – 660K, at respectively 525K, 581K, 632K and 659K are due to the evaporation of 2.78 remaining water molecules. The peaks at 525K and 581K are very intensive. It's worth noticing that the amount of water lost and the derived thermodynamic data make sense in view of the reactions with all the intermediate phases and intermediate products. In the first step, the weight loss is weak ($0.22H_2O$), that's why we observe only one peak in the DTG curve in this step. The reaction, according to Van Wazer [25], is:

$$Pb_3(P_3O_9)_2.3H_2O \longrightarrow (3PbO + 3P_2O_5 + 2.78H_2O)_{\text{Amorphous phase}} + 0.22H_2O_{(g)}$$

In the second step, the weight loss is important ($2.78H_2O$), that's why we observe four peaks in the DTG curve in this step. The reaction, according to Van Wazer [25], is:

$$(3PbO + 3P_2O_5 + 2.78H_2O)_{\text{Amorphous phase}} \longrightarrow 3\beta Pb(PO_3)_2 + 2.78H_2O_{(g)}$$

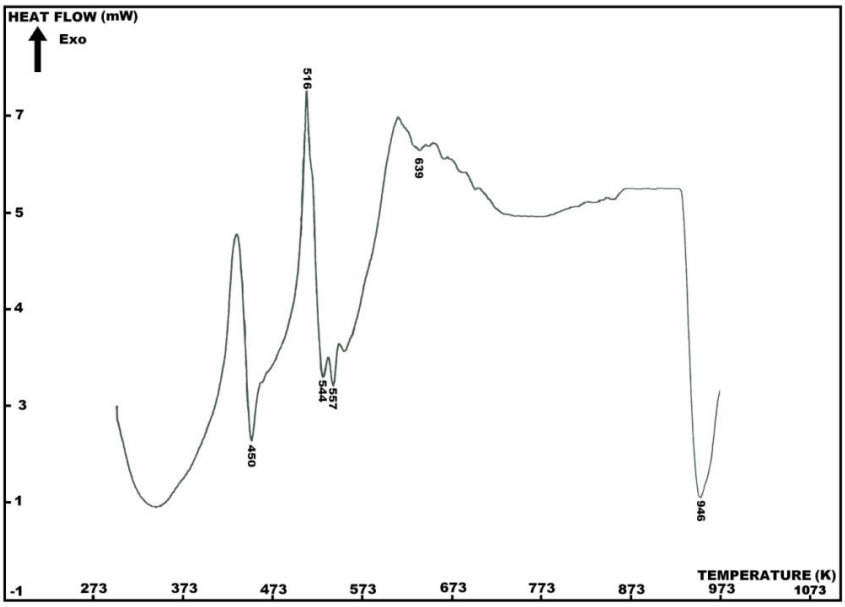

Figure 6. DTA curve of $Pb_3(P_3O_9)_2.3H_2O$ at rising temperature ($5K.min^{-1}$)

Fig. 6, which exhibits the differential thermal analysis (DTA) curve of $Pb_3(P_3O_9)_2.3H_2O$ under atmospheric pressure and at a heating rate $5K.min^{-1}$, reveals five endothermic effects and one exothermic. Four endothermic peaks, at 450K, 544K, 557K and 639K, are due to the departure of water molecules contained in the title compound. The first peak, well pronounced at 450K, corresponds to the loss of 0.22 water molecule. The second endothermic peak, dedoubled at 544K, the third at 557K and the fourth one at 639K are all due to the removal of 2.78 remaining water molecules. The exothermic peak at 516K is due to the crystallization of long-chain polyphosphate of lead. This crystallization is confirmed by X-ray diffraction and infrared spectrometry analyses. The last endothermic peak at 946K is due to the melting point of the long-chain polyphosphate $[Pb(PO_3)_2]_\infty$.

The differential scanning calorimetry, DSC, for $Pb_3(P_3O_9)_2.3H_2O$ at rising temperature $5K.min^{-1}$ and under atmospheric pressure shows one exothermic peak at 520K and five endothermic peaks at 445K, 462K**,** 607K, 620K and 661K **(Fig. 7)**.

The five endothermic peaks correspond to the dehydration of $Pb_3(P_3O_9)_2.3H_2O$ and are then due to the departure of water molecules. The only exothermic peak at 520K corresponds to the crystallization of long-chain polyphosphate of lead $[Pb(PO_3)_2]_\infty$ according to the results of $Cd_3(P_3O_9)_2.14H_2$[20,29]. In fact, in the results of M. H. Simont-Grange[29] and K. Sbai[20], the IR band appearing at 913 cm^{-1} in the spectrum of $Pb_3(P_3O_9)_2.3H_2O$, characterize easily the structure of long chain polyphosphates. This result is confirmed in the DTA curve by an exothermic peak at 516K. The enthalpy variations of the six peaks described above in the DSC curve are gathered in the **Table 4**.

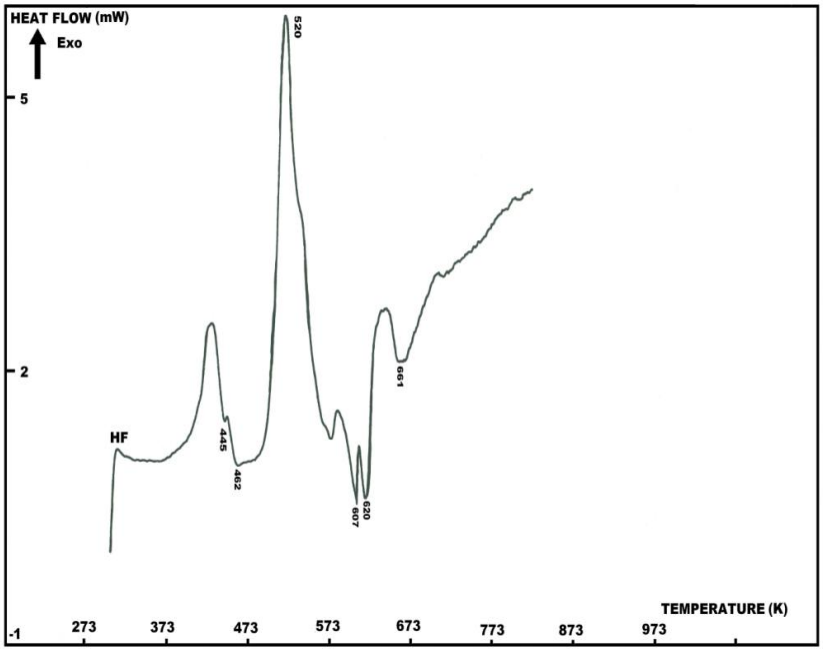

Figure 7. Differential scanning calorimetry DSC curve of $Pb_3(P_3O_9)_2.3H_2O$ at rising temperature ($5K.min^{-1}$)

The enthalpy variations were provided by the computer program. For the crystallization of $[Pb(PO_3)_2]_\infty$, we have the same temperatures for the exothermic peaks at 516K for the DTA curve and 520K for DSC curve. For the dehydration of $Pb_3(P_3O_9)_2.3H_2O$, we have approximately the same temperatures for the first and last endothermic peaks.

Table 4: Enthalpy variations and characteristic temperatures of the six peaks observed in the DSC curve of $Pb_3(P_3O_9)_2.3H_2O$ at rising temperature $5K.min^{-1}$

0.092 H_2O		0.129 H_2O		$[Pb(PO_3)_2]_\infty$		0.434 H_2O		0.462 H_2O		1.44 H_2O	
T_m	ΔH	T_m	ΔH	T_m	ΔH	T_m	ΔH	T_m	ΔH	T_m	ΔH
445	15.187	462	10.125	520	-53.934	607	20.308	620	40.070	661	32.930

T_m/K; ΔH/kJ.mol^{-1}

B. $Cd_3(P_3O_9)_2.14H_2O$

The two curves corresponding to the ATG and DTG analyses in air atmosphere and at a heating rate 10 $K.min^{-1}$ of $Cd_3(P_3O_9)_2.14H_2O$ are given in **Fig. 8**. The initial mass is 20mg. The dehydration of the cyclotriphosphate tetradecahydrate of cadmium $Cd_3(P_3O_9)_2.14H_2O$ occurs in three steps in three temperature ranges 345 – 446K, 446 – 586K and 586 – 703K **(Fig. 8).** In the thermogravimetric (ATG) curve **(Fig. 8)**, the first stage between 345 and 446K corresponds to the elimination of 11 water molecules, the second stage from 446 to 586K is due to the elimination of 2 water molecules and the third stage 586 – 703K corresponds to the elimination of one water molecule.

It is important to mention that the derivative of the ATG curve, DTG, of $Cd_3(P_3O_9)_2.14H_2O$ under atmospheric pressure and at a heating rate 10 K min^{-1} (**Fig. 8)** contains only three peaks due to the dehydration of $Cd_3(P_3O_9)_2.14H_2O$. The first intensive peak in the domain 345 – 446K, observed at 423K is due to the departure of 11 water molecules. The weak second peak in the domain 446 – 586K, observed at 523K is due to the departure of 2 water molecules and

the third peak in the third range 586 – 703K, situated at 675K is due to the removal of one water molecule.

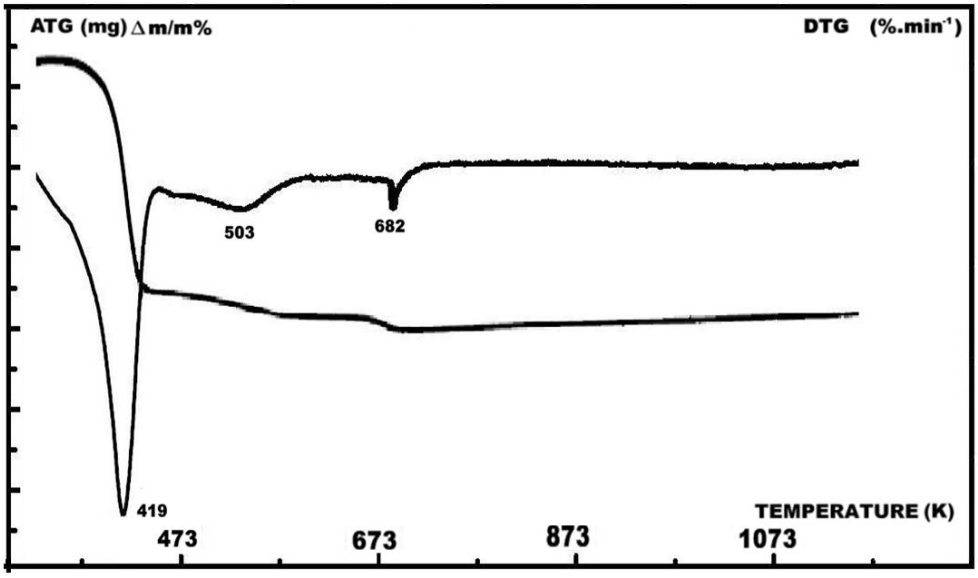

Figure 8. TGA (ATG-DTG) curves of $Cd_3(P_3O_9)_2.14H_2O$ at rising temperature (10K. min^{-1})

The differential thermal analysis (DTA) curve of $Cd_3(P_3O_9)_2.14H_2O$ **(Fig. 9)**, under atmospheric pressure and at a heating rate 10K.min^{-1}, reveals one exothermic peak and three endothermic effects. The exothermic peak at 707K is due to the crystallization of long-chain polyphosphate of cadmium form α. This crystallization, of $\alpha[Cd(PO_3)_2]$, is confirmed by X-ray diffraction and infrared spectrometry analyses. The first endothermic peak intensive at 421K corresponds to the loss of 11 water molecules. The second endothermic peak at 1120K is due to the phase transition from $\alpha[Cd(PO_3)_2]$ to $\beta[Cd(PO_3)_2]$ as proven by X-ray diffraction and infrared spectrometry analyses. The third endothermic peak at 1153K is rather related to the melting point of the long-chain polyphosphate $\beta[Cd(PO_3)_2]$.

The differential scanning calorimetry (DSC) curve of $Cd_3(P_3O_9)_2.14H_2O$, under atmospheric pressure and at a heating rate 10 K.min^{-1} **(Fig. 9)**, shows three endothermic peaks at 419K, 503K and 682K. All of these peaks correspond to the dehydration of $Cd_3(P_3O_9)_2.14H_2O$.

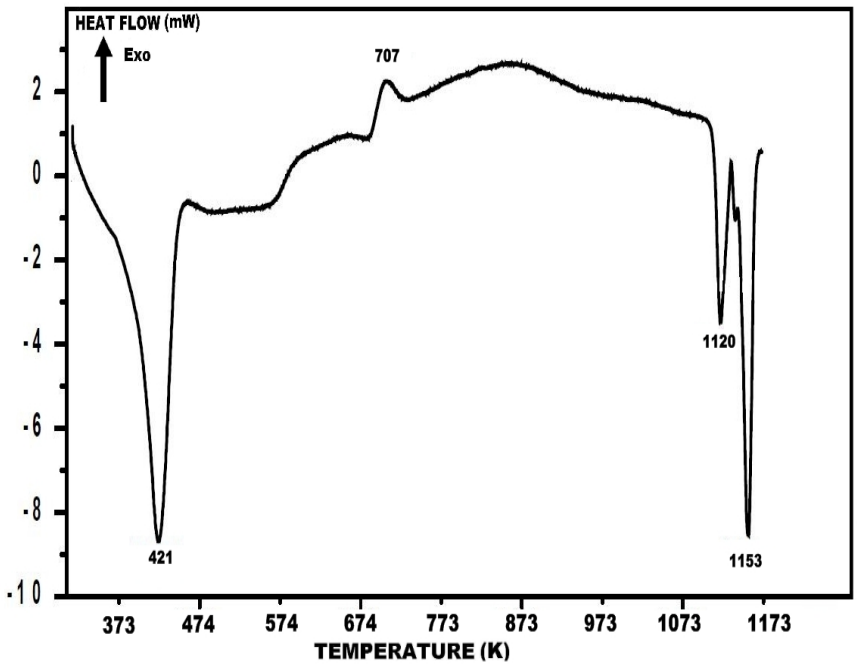

Figure 9. DTA curve of $Cd_3(P_3O_9)_2.14H_2O$ at rising temperature ($10K.min^{-1}$)

The enthalpy variations of the three peaks described above in the DSC curve are gathered in the **Table 5.** concerning the dehydration of $Cd_3(P_3O_9)_2.14H_2O$, we have the same temperatures for the endothermic peaks at 421K for the DTA curve and 419K for DSC curve **(Fig. 10).**

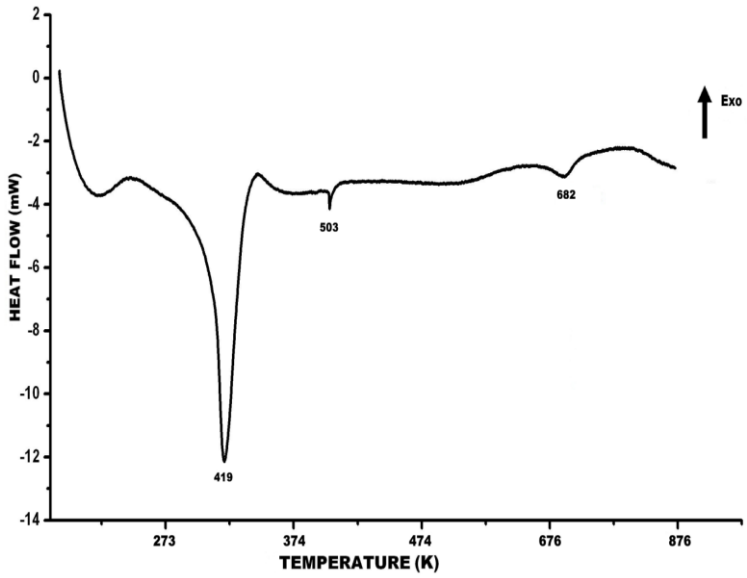

Figure 10. Differential scanning calorimetry DSC curve of $Cd_3(P_3O_9)_2.14H_2O$ at rising temperature ($10K.min^{-1}$)

Table 5 Enthalpy variations and characteristic temperatures of the three peaks observed in the DSC curve of $Cd_3(P_3O_9)_2.14H_2O$ at rising temperature $10K.min^{-1}$

11 H_2O		2 H_2O		1 H_2O	
T_m	ΔH	T_m	ΔH	T_m	ΔH
419	954.73	503	7.2936	682	38.227

T_m/K; ΔH/kJ.mol^{-1}

Estimation of the thermodynamic functions.

Various equations of kinetic analyses are known such as Kissinger's method[30], Kissinger-Akahira-Sunose (KAS)[31], Ozawa[32], Coats-Redfern[33] and Van Krevelen et al.[34] methods. Especially, the Ozawa and KAS equations were well described and widely used in the literature; therefore, these methods are selected in studying the kinetics of thermal dehydration of the title compounds. So, water loss kinetic parameters were evaluated using the Kissinger-Akahira-Sunose (KAS)[31] and Ozawa[32] methods, from the curves $\ln(v/T^2_m) = f(1/Tm)$ and $\ln(v) = f(1/T_m)$ (**Fig. 11, 12, 13** and **14**),where v is the heating rate and T_m the sample temperature at the thermal effect maximum. The characteristic temperatures at maximum dehydration rates, T_m, for the cyclotriphosphates $Pb_3(P_3O_9)_2.3H_2O$ and $Cd_3(P_3O_9)_2.14H_2O$ are shown in **Table 6**. The enthalpy variations were provided by the DSC apparatus.

Table 6 Characteristic temperatures at maximum dehydration rates, T_m in K, at different heating rates from the DTA curves of $Pb_3(P_3O_9)_2.3H_2O$ and $Cd_3(P_3O_9)_2.14H_2O$

$Pb_3(P_3O_9)_2.3H_2O$					
Heating rate v	3K/min	5K/min	8K/min	10K/min	13K/min
First peak	439	450	462	473	480
Second peak	525	544	553	564	568
Third peak	544	557	568	575	602
Fourth peak	625	639	652	667	679
$Cd_3(P_3O_9)_2.14H_2O$					
Heating rate v	5K/min	10K/min	15K/min		
One peak	418	420	422		

From these temperatures and according to the Kissinger-Akahira-Sunose (KAS)[31] and Ozawa[32] methods, the apparent activation energies of dehydration were calculated for the cyclotriphosphates $Pb_3(P_3O_9)_2.3H_2O$ and $Cd_3(P_3O_9)_2.14H_2O$ (**Table 7**). For the Kissinger-Akahira-Sunose (KAS)[31] method, the slope of the resulting straight line of the curve: $\ln(v/T^2m) = f(1/Tm)$ (**Fig. 11** and **13**), equals to -Ea/R, allows the apparent activation energy to be calculated (**Table 7**).

Table 7: Activation energy values Ea, pre-exponential factor (A) and correlation coefficient (r^2) calculated by Ozawa and KAS methods for the dehydration of $Pb_3(P_3O_9)_2.3H_2O$ and $Cd_3(P_3O_9)_2.14H_2O$

$Pb_3(P_3O_9)_2.3H_2O$						
Model	Ozawa method			KAS method		
	Ea /kJ. mol^{-1}	A.10^{11}/min^{-1}	r^2	Ea/kJ. mol^{-1}	A.10^{5}/min^{-1}	r^2
First peak	61.93	13.72	0.985	57.50	7.78	0.974
Second peak	83.74	171.5	0.950	78.98	69.8	0.938
Third peak	73.00	7.423	0.941	67.25	2.68	0.966
Fourth peak	96.55	118.8	0.974	90.71	33.8	0,979

$Cd_3(P_3O_9)_2.14H_2O$						
Model	Ozawa method			KAS method		
	Ea / kJ. mol^{-1}	A.10^{12}/ min^{-1}	r^2	Ea / kJ. mol^{-1}	A.10^{5} / min^{-1}	r^2
One peak	55.39	1.278	0.978	51.25	8.58	0.972

Concerning the Ozawa[32] method, the slope of the resulting straight line on the curve: ln(v) = f(1/Tm) (**Fig. 12** and **14**), equals to -1.0516E/R, allows also the apparent activation energy (**Table 7**) to be calculated by this second way. The equations used for the two methods are the following :

For KAS[31]

$$Ln\left(\frac{v}{T^2{}_m}\right) = Ln\left(\frac{AR}{E}\right) - \left(\frac{E}{R}\right)\left(\frac{1}{T_m}\right) \quad (1)$$

For Ozawa[32]

$$Ln(v) = Ln\left(\frac{AR}{1.0516E}\right) - 1.0516\left(\frac{E}{R}\right)\left(\frac{1}{T_m}\right) \quad (2)$$

The pre-exponential factor or Arrhenius constant (A) can be calculated from both KAS[30] and Ozawa[32] methods. The related thermodynamic functions can be calculated by using the activated complex theory (transition state) of Eyring[35-37]. The following general equation can be written[36]:

$$A = \left(\frac{e\chi\, k_B T_m}{h}\right) exp\left(\frac{\Delta S^*}{R}\right) \quad (3)$$

where e is the Neper number (e = 2.7183), χ is the transition factor, which is unity for the monomolecular reaction, k_B is the Boltzmann constant (k_B = 1.3806 × 10^{-23} $J.K^{-1}$), h is Plank's constant (h = 6.6261 × 10^{-34} J.s), Tm is the peak temperature of the DTA curve, R is the gas constant (R = 8.314 $J.K^{-1}.mol^{-1}$) and ΔS* is the entropy change of transition state complex or entropy of activation. Thus, the entropy of activation may be calculated as follows:

$$\Delta S^* = RLn\frac{Ah}{e\chi\, k_B T_m} \quad (4)$$

The enthalpy change of transition state complex or heat of activation (ΔH*) and Gibbs free energy of activation (ΔG*) of dehydration were calculated according to Eqs. (5) and (6), respectively:

$$\Delta H^* = E^* - RT \quad (5)$$

$$\Delta G^* = \Delta H^* - \Delta S^* T_m \quad (6)$$

Where, E* is the activation energy Ea of both KAS[31] and Ozawa[32] methods. The values of the activation energies are gathered in **Table 7**. Thermodynamic functions were calculated from Eqs. (4), (5) and (6) and summarized in **Table 8**. The negative values of ΔS* from two methods for the dehydration step reveals that the activated state is less disordered compared to the initial state. These ΔS* values suggest a large number of degrees of freedom due to rotation which may be interpreted as a « slow » stage[37-39] in this step. The positive values of ΔG* at all studied methods are due to the fact that, the dehydration processes are not spontaneous. The positivity of ΔG* is controlled by a small activation entropy and a large positive activation enthalpy according to the Eq. 6. The endothermic peaks in DTA data agree well with the positive sign of the activation enthalpy (ΔH*). The estimated thermodynamic functions ΔS* and ΔG* (**Table 8**) from two methods are different to some extent due to the different pre-exponential factor of about 10^6 or 10^7. While ΔH* (**Table 8**) exhibits an

independent behavior on the pre-exponential factor as seen from exhibiting nearly the same value.

Table 8: Values of ΔS*, ΔH* and ΔG* for dehydration step of $Pb_3(P_3O_9)_2.3H_2O$ and $Cd_3(P_3O_9)_2.14H_2O$ calculated according to Ozawa and KAS equations

$Pb_3(P_3O_9)_2.3H_2O$						
Model	Ozawa method			KAS method		
	ΔS* (J. $K^{-1}.mol^{-1}$)	ΔH* ($kJ.mol^{-1}$)	ΔG* ($kJ.mol^{-1}$)	ΔS* (J. $K^{-1}.mol^{-1}$)	ΔH* ($kJ.mol^{-1}$)	ΔG* ($kJ.mol^{-1}$)
First peak	-24.83	57.94	69.86	-144.41	53.51	122.82
Second peak	-5.23	79.02	81.99	-127.57	74.62	146.72
Third peak	-31.81	68.00	87.13	-155.13	62.25	155.56
Fourth peak	-9.77	90.91	97.54	-135.73	85.06	176.78
$Cd_3(P_3O_9)_2.14H_2O$						
Model	Ozawa method			KAS method		
	ΔS* (J. $K^{-1}.mol^{-1}$)	ΔH* ($kJ.mol^{-1}$)	ΔG* ($kJ.mol^{-1}$)	ΔS* (J. $K^{-1}.mol^{-1}$)	ΔH* ($kJ.mol^{-1}$)	ΔG* ($kJ.mol^{-1}$)
One peak	-24.34	51.88	62.16	-142.52	47.74	107.88

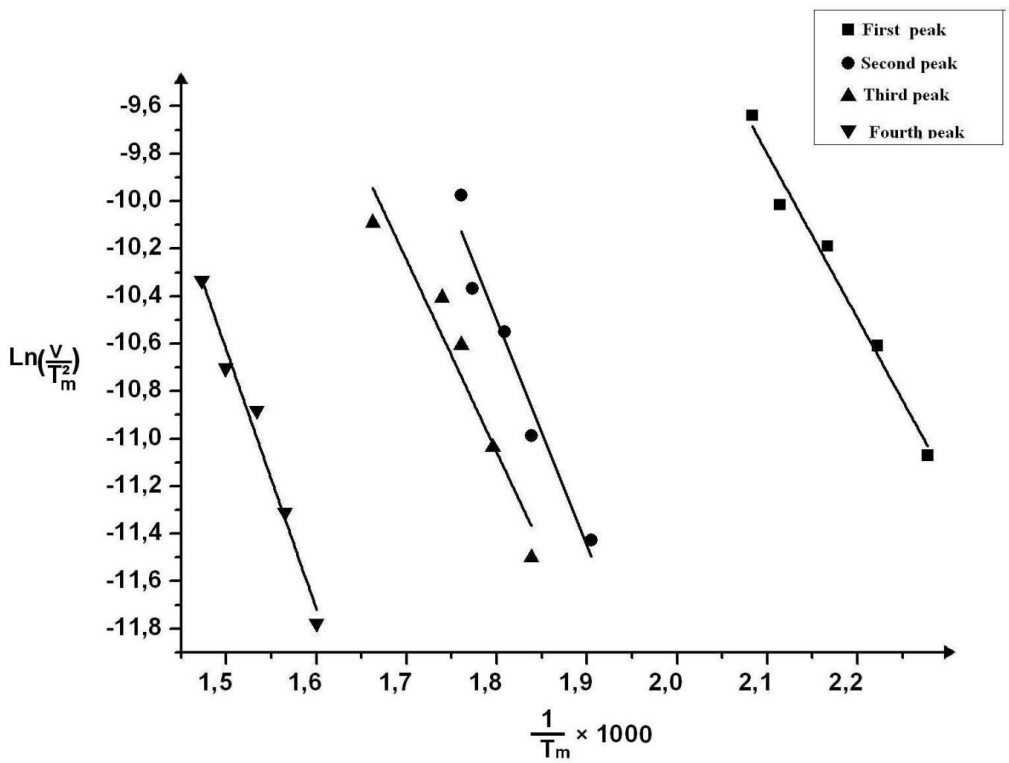

Figure 11. $Ln(v/T_m^2) = f(1/T_m)$ representation of the dehydration thermal effect of the cyclotriphosphate $Pb_3(P_3O_9)_2.3H_2O$

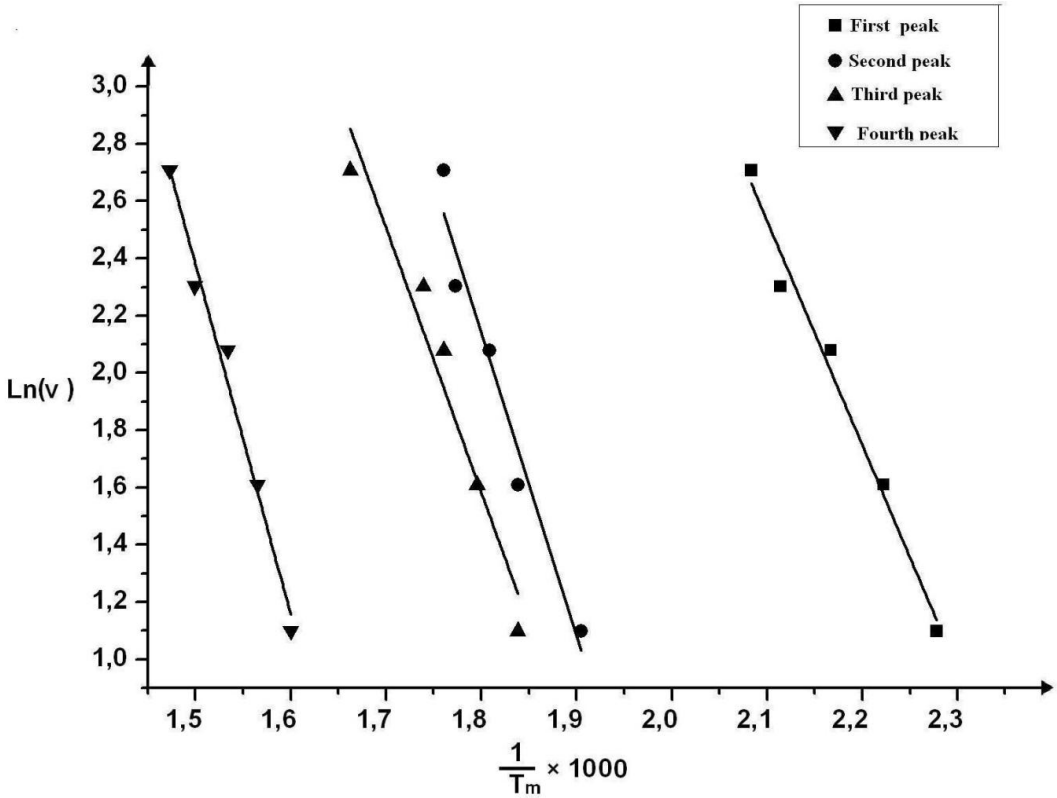

Figure 12. Ln(v) = f(1/T_m) representation of the dehydration thermal effect of the cyclotriphosphate $Pb_3(P_3O_9)_2.3H_2O$

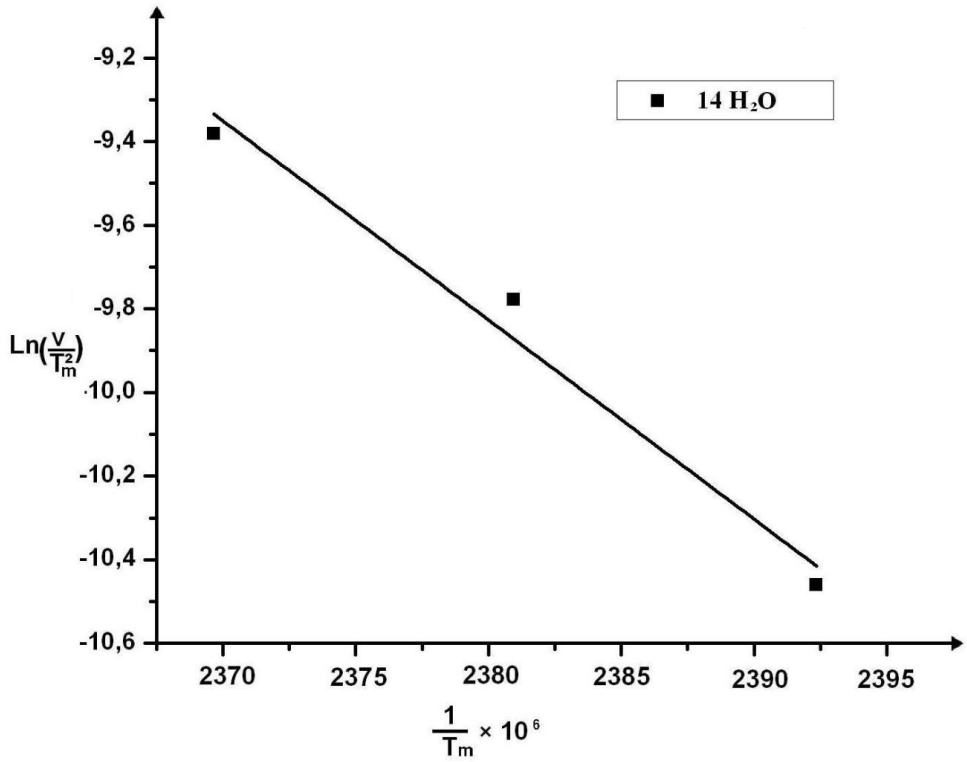

Figure 13. Ln(v/T_m^2) = f(1/T_m) representation of the dehydration thermal effect of the cyclotriphosphate $Cd_3(P_3O_9)_2.14H_2O$

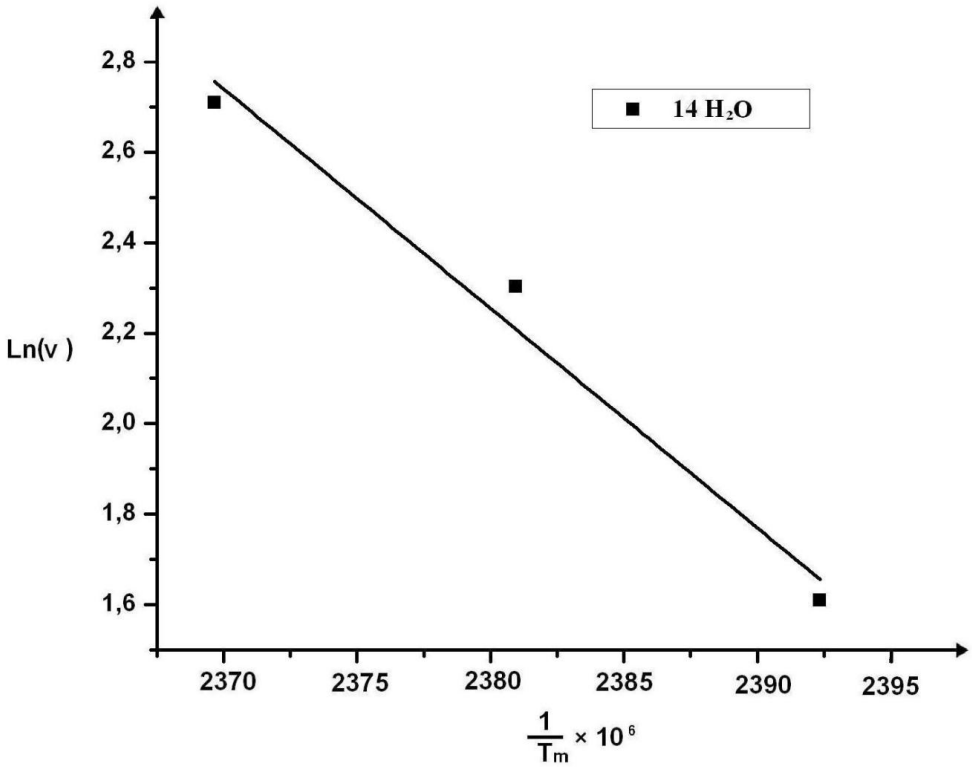

Figure 14. Ln(v) = f(1/T_m) representation of the dehydration thermal effect of the cyclotriphosphate $Cd_3(P_3O_9)_2.14H_2O$

Comparison of the thermal behavior of cyclotriphosphates hydrated type $M_3^{II}(P_3O_9)_2.10H_2O$ (M^{II} = Ca, Mn and Cd) and $Ba_3(P_3O_9)_2.6H_2O$ with that of $Pb_3(P_3O_9)_2.3H_2O$ and $Cd_3(P_3O_9)_2.14H_2O$.

In our laboratory, until today, the thermal behavior was studied for four cyclotriphosphates hydrated type $M^{II}_3(P_3O_9)_2.10H_2O$ (M^{II} = Ca, Mn and Cd)[16,40] and $Ba_3(P_3O_9)_2.6H_2O$[41]. It would be useful to compare the thermal behavior of these four cyclotriphosphates with that of $Pb_3(P_3O_9)_2.3H_2O$ and $Cd_3(P_3O_9)_2.14H_2O$. For the cyclotriphosphates $M_3^{II}(P_3O_9)_2.10H_2O$ (M^{II} = Ca, Mn and Cd)[16,40], $Ba_3(P_3O_9)_2.6H_2$[41], $Pb_3(P_3O_9)_2.3H_2O$ and $Cd_3(P_3O_9)_2.14H_2O$, after the removal of a partial quantity of water molecules by thermal dehydration, they all lead to amorphous products in X-ray diffraction and don't exhibit the IR absorption bands characteristic of cyclic phosphates $P_3O_9^{3-}$. The final products of the total thermal dehydration, for $Ca_3(P_3O_9)_2.10H_2O$[16,40], $Ba_3(P_3O_9)_2.6H_2O$[41], $Pb_3(P_3O_9)_2.3H_2O$ and $Cd_3(P_3O_9)_2.14H_2O$, are their corresponding long-chain polyphosphates $[M^{II}(PO_3)_2]_\infty$ (M^{II} = Ca, Ba, Pb and Cd) except for $Mn_3(P_3O_9)_2.10H_2O$[16] and $Cd_3(P_3O_9)_2.10H_2O$[16] which lead to their corresponding anhydrous cyclotetraphosphates respectively $Mn_2P_4O_{12}$[16] and $Cd_2P_4O_{12}$[16]. These results are gathered in **Table 9.**

Table 9: Comparison of the thermal behaviors of $Pb_3(P_3O_9)_2.3H_2O$ and $Cd_3(P_3O_9)_2.14H_2O$ with those of $Ba_3(P_3O_9)_2.6H_2O$, $Ca_3(P_3O_9)_2.10H_2O$, $Cd_3(P_3O_9)_2.10H_2O$ and $Mn_3(P_3O_9)_2.10H_2O$

cyclotriphosphates	first step : dehydration	second step : melting or phase transition	last step : melting	References
$Pb_3(P_3O_9)_2.3H_2O$	Formation of $[Pb(PO_3)_2]$ between 593 and 773K	Melting of $[Pb(PO_3)_2]$ at 946K		This work
$Cd_3(P_3O_9)_2.14H_2O$	Formation of $\alpha[Cd(PO_3)_2]$ between 500 and 1073K	Formation of $\beta[Cd(PO_3)_2]$ between 830 and 1133K	Melting of $\beta[Cd(PO_3)_2]$ at 1153K	This work
$Ba_3(P_3O_9)_2.nH_2O$ (n = 4, 6)	Formation of $\beta[Ba(PO_3)_2]$ between 500 and 973K	Melting of $\beta[Ba(PO_3)_2]$ at 1143K		41, 42
$Ca_3(P_3O_9)_2.10H_2O$	Formation of $\beta[Ca(PO_3)_2]$ between 773 and 923K	Melting of $\beta[Ca(PO_3)_2]$ at 1370K		16, 40
$Mn_3(P_3O_9)_2.10H_2O$	Formation of $Mn_2P_4O_{12}$ between 320 and 1243K	Melting of $Mn_2P_4O_{12}$ at 1373K		16, 40
$Cd_3(P_3O_9)_2.10H_2O$	Formation of $Cd_2P_4O_{12}$ between 320 and 1243	Melting of $Cd_2P_4O_{12}$ at 1373K		16, 40

Conclusion

$Pb_3(P_3O_9)_2.3H_2O$ has been synthesized by mixing $Pb(NO_3)_2$ and $Na_3P_3O_9$ in aqueous solution and $Cd_3(P_3O_9)_2.14H_2O$ has been prepared by the method of ion exchange-resin. The total thermal dehydration of $Pb_3(P_3O_9)_2.3H_2O$ under atmospheric pressure leads to the long-chain polyphosphate, $[Pb(PO_3)_2]_\infty$. With further increase in temperature, finally, $[Pb(PO_3)_2]_\infty$ melts at 946K. The thermal dehydration of $Cd_3(P_3O_9)_2.14H_2O$, under atmospheric pressure, leads to its long chain polyphosphate form α, $\alpha[Cd(PO_3)_2]_\infty$ as an intermediate product. By heating at higher temperatures, $\alpha[Cd(PO_3)_2]_\infty$ converts to the long-chain polyphosphate form β, $\beta[Cd(PO_3)_2]_\infty$. $\beta[Cd(PO_3)_2]_\infty$ which is the final product of dehydration, is stable until its melting point at 1153K. The thermodynamic and kinetic features of the dehydration of $Pb_3(P_3O_9)_2.3H_2O$ and $Cd_3(P_3O_9)_2.14H_2O$ have been determined. The vibrational spectra of $Pb_3(P_3O_9)_2.3H_2O$ and $Cd_3(P_3O_9)_2.14H_2O$ were examined and interpreted in the domain of the stretching vibrations of the P_3O_9 rings. $Pb_3(P_3O_9)_2.3H_2O$, $Cd_3(P_3O_9)_2.14H_2O$, $Ca_3(P_3O_9)_2.10H_2O$ and $Ba_3(P_3O_9)_2.6H_2O$ have the same thermal behavior. They all lead to their corresponding long-chain polyphosphates $[M^{II}(PO_3)_2]_\infty$ (M^{II} = Pb, Cd, Ca and Ba).

On the contrary, $Mn_3(P_3O_9)_2.10H_2O$ and $Cd_3(P_3O_9)_2.10H_2O$ lead to their corresponding cyclotetraphosphates $M^{II}{}_2P_4O_{12}$ (M^{II} = Mn, Cd). The results presented in this paper can be added to previous works on thermal transformations of condensed hydrated cyclophosphates.

Experimental Section

X-ray diffraction.

Powder diffraction patterns were registered with a Siemens Chemical analyses diffractometer type D5000 using CuKλ radiation (λ = 1.5406Å). Chemical analyses were performed on a spectrophotometer of atomic absorption type VARIAN AA-475.

Infrared spectroscopy. Spectra were recorded in the range 4000-400 cm^{-1} with a Perkin-Elmer IR 983G spectrophotometer, using samples dispersed in spectroscopically pure KBr pellets and in the range 600-30 cm-1 with Bruker IFS66V/S spectrophotometer.

Thermal analyses. TGA-DTA coupled were performed using the multimodule 92 Setaram analyzer operating from room temperature up to 1673K, in a platinum crucible and in atmospheric pressure with sample mass: 20.00mg, at various heating rates from 1 to 15K/min.

Differential scanning calorimetry (DSC) was carried out with a Setaram DSC 92 apparatus, in a platinum crucible and in atmospheric pressure with sample mass: 20.00mg.

References

1 - M. T. Averbuch-Pouchot, A. Durif, Z. Kristallogr. **1972**,135, 318-319
2 - M. T. Averbuch-Pouchot, A. Durif, I. Tordjman, Crys. Struct. Comm. **1973**, 2, 89-90.
3 - M. T. Averbuch-Pouchot, A. Durif, J. C. Guitel, Acta Crystallogr. **1976**, B32, 1533-1535.
4 - M. T. Averbuch-Pouchot, A. Durif, J. C. Guitel, Acta Crystallogr. **1976**, B32, 1894-1896.
5 - N. EL-Horr , A. Durif, C. R. Acad. Sci. Ser. II **1983**, 296, 1185-1187.
6 - A. Durif, M. Bagieau-Beucher, C. Martin, J. C. Grenier, Bull. Soc. Fr. Mineral. Cristallogr. **1972**, 95, 146-148.
7 - I. Trodjman, A. Durif, J. C. Guitel, Acta Crystallogr B. **1976**, 32, 205-208.
8 - J. C. Grenier, C. Martin, Bull. Soc. Fr. Mineral. Cristallogr. **1975**, 98, 107-110.
9 - R. Masse, J. C. Guitel, A. Durif, Acta Crystallogr. **1976**, B32, 1892-1894.
10 - M. T. Averbuch-Pouchot, A. Durif, Z. Kristallogr. **1986**, 174, 219-224.
11 - A. Durif, M. Brunel-Laügt, J. Appl. Crystallogr. **1976**, 9, 154-156.
12 - M. Brunel-Laügt, I. Trodjman, A. Durif, Acta Crystallogr. **1976**, B32, 3246-3249.
13 - M. T. Averbuch-Pouchot, A. Durif, Topics in Phosphate Chemistry, World Scientific Publishing Co. Singapore, New Jersey, London, Hong Kong, **1996**.
14 - A. Durif, Crystal Chemistry of Condensed Phosphates, Plenum Press, New York, **1995**.
15 - K. Sbai, A. Abouimrane, K. El Kababi, S. Vilminot, J. Therm. Anal. Cal. **2002**, 68, 109-122.
16 - K. Brouzi, A. Ennaciri, M. Harchrras, K. Sbai, Ann. Chim. Sci. Mat. **2003,** 28, 159-166.
17 - R. Dumon, Le Phosphore et les Composés Phosphorés, Masson Paris New York Barcelone Milan, **1980**.
18 - M. Greenblatt, P. P. Tsai, T. Kodama, S. Tanase, Solid State Ionics **1990**, 40/41, 444-447.
19 - A. Jouini, A. Durif, C. R. Acad. Sci. Paris. **1983**, 297II, 573-575.
20 - K. Sbai, A. Atibi, A. Charaf, M. Radid, A. Jouini, J. Therm. Anal. Cal., **2002**, 69, 627-645.
21 - W. Bues und, H. W. Gerhke, Anorg. Z. Allgem. Chem. **1956**, 288, 301-307.

22 - P. Tarte, A. Rulmont, K. Sbai , M. H. Simonot-Grange. Spectrochimica Acta, **1987**, 43A(3), 337-345.
23 - K. Sbai, A. Abouimrane, A. Lahmidi, K. El Kababi, M. Hliwa , S. Vilminot, Ann. Chim. Sci. Mat,. **2000**, 25(1), S139-S143.
24 - M. H. Simonot-Grange, J. Sol. State Chem. **1983,** 46, 76-86.
25 - J. R. Van Wazer, K. A. Holst, J. Am. Chem. Soc. **1950**, 72(2)**,** 639-644.
26 - K. H. Jost, Acta Crystallogr. **1964**, 17, 1539-1544.
27 - M. Bagieu-Beucher, J. C. Guitel, I. Tordjman, A. Durif, Bull Soc Fr. Mineral Cristallogr. **1974**, 97, 481-484.
28 - M. Bagieu-Beucher, M. Brünel-Laügt, J. C. Guitel, Acta Crystallogr. Sect B, **1979**, 35, 292-295.
29 - M. Thilo, I. Grunze, Z. Anorg. Allg. Chem. **1957,** 90(5-6**)**, 209-223.
30 - H. E. Kissinger, Ann. Chem. **1957**, 29, 1702-1709.
31 - T. Akahira, T. Sunose, Res. Report Chiba Inst. Techno. **1971**, 16, 22-25.
32 - T. Ozawa, Bull. Chem. Soc. Jpn. **1965**, 38, 1881-1886.
33 - A.W. Coats, J.P. Redfern, Nature **1964**, 201(4914), 68–69.
34 - D. W. Van Krevelns, P. J. Hoftijzer, Trans. Inst. Chem. Eng. **1954**, 32, 5360-5365.
35 - D. Young, Decomposition of solids, Academia Prague, **1984**.
36 - J. J. Rooney, J. Mol. Catal. A. Chem., **1995**, 96(1), L1-L3'
37 - B. Boonchom, J. Chem. Eng. Data **2008**, 53(7), 1533-1541.
38 - L. Vlaev, N. Nedelchev, K. Gyurova, M. Zagorcheva, J. Anal. Appl. Pyrol. **2008**, 81(2), 253-262.
39 - P. Noisong, C. Danvirutai, T. Boonchom, Sol. State Sci. **2008**, 10(11), 1598-1603.
40 - S. Belaaouad, M. Tridane, H. Chennak, R. Tamani, A. Kenz , M. Moutaabbid, Phos. Res. Bull. **2007**, 21, 60-70.
41 - S. Belaaouad, Y. Lahrir, S. Sarhane , M. Tridane, Phos. Res. Bull. **2009**, 23, 67-75.
42- A. Kheïreddine, M. Tridane and S. Belaaouad, Powder Diffraction. **2012,** 27 (1), 32-35.